Carrier-carrier scattering in GaAs/Al_xGa_{1-x}As quantum wells

K. W. Sun* and T. S. Song
Department of Electronic Engineering, Feng Chia University, Taichung, Taiwan, Republic of China

C.-K. Sun and J. C. Wang
Department of Electrical Engineering and Graduate Institute of Electro-Optical Engineering, National Taiwan University, Taipei, Taiwan, Republic of China

M. G. Kane
Sarnoff Corporation, Princeton, New Jersey 08543

S. Y. Wang and C. P. Lee
Department of Electronics Engineering and Institute of Electronics, National Chiao Tung University, Hsin Chu, Taiwan, Republic of China

(Received 7 December 1999; revised manuscript received 14 March 2000)

We have studied carrier dynamics in highly nonequilibrium two-dimensional (2D) carrier distributions generated with femtosecond laser pulses in *p*-doped GaAs/$Al_{0.32}Ga_{0.68}$As quantum wells at photoexcited carrier densities between 10^9 and $10^{11}\,cm^{-2}$. The initially nonthermal carrier distribution is quickly broadened due to inelastic carrier-carrier scattering, with the broadening rate increasing as carrier density is increased. Measurements of the unrelaxed peak height in the hot electron-neutral acceptor luminescence spectra are compared with calculations of the carrier distribution using integration of the 2D dynamically screened Boltzmann equation. Our results indicate that carrier-carrier scattering becomes as significant a scattering mechanism as LO-phonon emission at density of about $10^{10}\,cm^{-2}$.

I. INTRODUCTION

Femtosecond optical spectroscopy has proven to be a very useful tool for the study of fundamental nonequilibrium properties in semiconductors.[1–9] Femtosecond excitation of GaAs can generate an initial highly nonequilibrium electron distribution, which then thermalizes to an equilibrium distribution by carrier-carrier interactions and phonon emission. Thermalization times of 50 to 300 fsec have been deduced from hole burning in transient absorption spectra for excitation below the optical-phonon energy.[3–5] Luminescence upconversion experiments reveal the rapid redistribution of electrons and holes over a wide energy range within the first 100 fsec after excitation at densities larger than $10^{17}\,cm^{-3}$, demonstrating the dominant role of carrier-carrier scattering at these carrier densities.[8] Carrier-carrier interactions among highly nonequilibrium photoexcited carriers in GaAs have been studied at injected carrier densities from 10^{15} to $10^{17}\,cm^{-3}$ in Refs. 2, 10, and 11. The rate of carrier-carrier scattering within the highly nonequilibrium distribution created by laser excitation is comparable to the LO-phonon emission rate of approximately 1/(150 fsec) (Refs. 12–15) at a carrier density of about $10^{16}\,cm^{-3}$.

While there are still questions remaining, it appears safe to say that hot electron relaxation in bulk GaAs is relatively well understood. However, in 2D the situation is unclear. Less experimental data on carrier-carrier scattering rates are available for 2D carriers than 3D carriers. Kash has studied the energy loss rate of a hot electron to a thermalized electron-hole plasma in GaAs/Al_xGa_{1-x}As quantum wells.[16] Knox and co-workers studied scattering among 2D carriers in a nonthermal distribution.[4,17,18] They found that at an injected carrier density of $2\times10^{10}\,cm^{-2}$ in undoped quantum wells electrons scatter out of the initial distribution in about 100 fsec and form a thermal distribution in about 200 fsec. Kane calculated 2D carrier-carrier scattering rates and found qualitative agreement with the results of Knox and co-workers.[19]

In this report we have made time-resolved measurements of the electron distribution at densities between 10^9 and $10^{11}\,cm^{-2}$. We excited the sample with an ultrafast optical pulse and measured the time-integrated hot electron to neutral acceptor [hot(e,Å)] luminescence spectrum as a function of photoexcited carrier density. We are able to create a highly nonequilibrium distribution of energetic carriers because the 120 fsec laser pulses are shorter than the LO-phonon emission time (~150 fsec).[20–25] By measuring the height of the first unrelaxed peak in the hot(e,Å) luminescence spectra, we are able to sample the electron distribution within an LO-phonon emission time.

II. EXPERIMENTAL RESULTS

The MQW samples studied here were 5 nm GaAs wells with 25 nm thick $Al_{0.32}Ga_{0.68}$As barriers. The quantum wells were *p*-doped with Be at a density of $10^{18}\,cm^{-3}$ in the central 1 nm of each well. The quantum well samples consisted of a stack of 40 wells and were grown on [100] undoped GaAs substrates. For all experiments reported here, the samples were held in a closed-cycle cryostat refrigerator at $T=10\,K$ to ensure that virtually all the acceptors were neutral and to reduce the equilibrium LO-phonon occupancy to insignificant levels. The hot(e,Å) luminescence spectra are taken with a SPEX Triplemate spectrometer and a liquid-nitrogen

0163-1829/2000/61(23)/15592(4)/$15.00
©2000 The American Physical Society

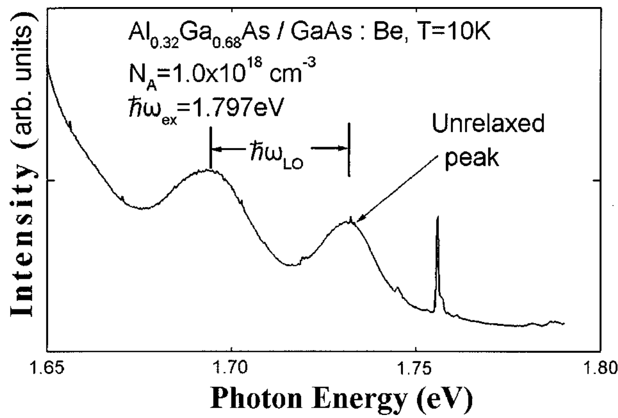

FIG. 1. Time-integrated luminescence spectrum of GaAs quantum wells during cw excitation at 1.797 eV. The carrier density is low. The peak at 1.73 eV corresponds to electrons that have been excited to the lowest conduction subband from the lowest heavy-hole subband, and have recombined with neutral acceptors without emitting an LO phonon.

cooled CCD detector. The experiments have employed two excitation sources–an argon ion laser-pumped cw dye laser and a self-mode-locked Ti:sapphire laser. The cw dye laser was operated at an energy of 1.797 eV, and the self-mode-locked Ti:sapphire laser, which generated 120 fsec optical pulses at a 80 MHz repetition rate, was operated at the same energy. An optical multichannel analyzer was used to monitor the laser pulse width throughout the experiments.

Figure 1 shows the time-integrated luminescence spectrum with the dye laser used to excite a low carrier density. The sharp peak at 1.756 eV and shoulder at 1.745 eV in Fig. 1 are first-order Raman peaks from photon scattering with GaAs-like and $Al_xGa_{1-x}As$-like LO phonons. These peaks will not be analyzed here. In Fig. 1, the peak at 1.73 eV is the unrelaxed peak due to electrons that have been excited by the laser pulse to the lowest conduction subband from the lowest heavy-hole subband by the laser pulse and have recombined with neutral acceptors. The peak below this one at 1.695 eV is a superposition of a peak due to electrons excited from the heavy-hole subband that have emitted one 37 meV LO phonon, and electrons excited from the lowest light-hole subband. Nevertheless, the well-defined higher peak at 1.73 eV demonstrates that 2D photoexcited electrons relax through successive LO-phonon emission events before recombining with neutral acceptors.

In Fig. 2 we show spectra obtained using a self-mode-locked Ti:sapphire laser as the excitation source. By defocusing the laser, the injected carrier density was varied from 10^9 to $10^{11}\,cm^{-2}$. Using a periscope arrangement behind the entrance slit in the spectrometer, the photoexcited carrier densities are determined from the laser spot size on the sample and the absorption coefficient of the QW samples at the excitation wavelength. Our detection system is adjusted to sample only the central half of the laser spot, thus minimizing uncertainties associated with non-uniform injection. We have also compared our estimated carrier densities with those obtained in differential-transmission type experiments,[4,16–18] in which the absorption depth can be accurately determined, and our estimate of the injected carrier densities agrees within a factor of 2. (Carrier diffusion can be ignored on a femtosecond time scale.)

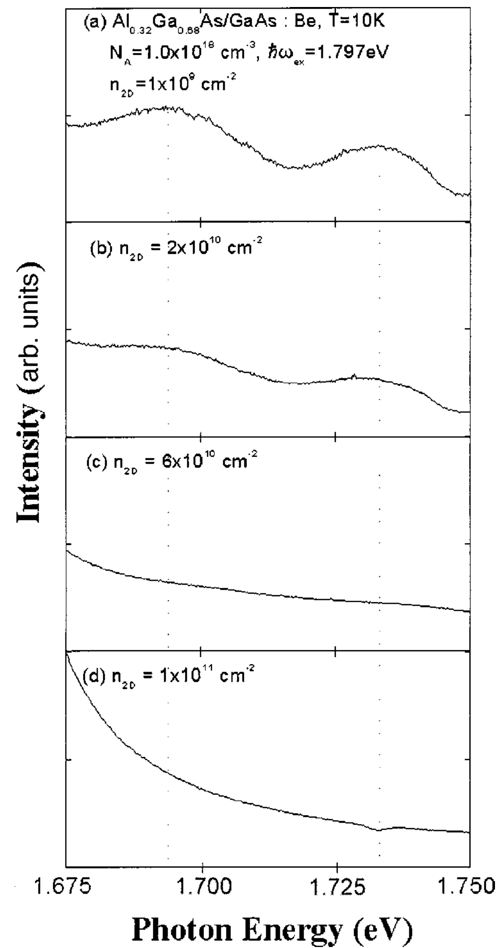

FIG. 2. Time-integrated luminescence spectrum of GaAs quantum wells excited by 120 fsec pulses at varying carrier densities. Carrier-carrier scattering causes the peaks to disappear as the carrier density is increased.

The spectra for injected carrier densities from 10^9 to $10^{11}\,cm^{-2}$ are shown in Figs. 2(a)–2(d). The unrelaxed peak begins to decrease at carrier densities above $10^9\,cm^{-2}$. As the injected carrier density is increased to $10^{11}\,cm^{-2}$, the peaks disappear. The unrelaxed peak corresponds to the electron distribution near the initial energy during the first 150 fsec (the LO-phonon emission time), convolved with density-independent broadening mechanisms such as acceptor-acceptor interactions. We find no change in the linewidth of the peak, and thus measurements of the integrated area under the peak give the same results as measuring the peak height. In Fig. 3 we plot the unrelaxed peak intensity relative to the background (which remains relatively constant) in each spectrum as a function of injected carrier density. The probability is small that an electron will be scattered out of this peak before emitting a LO phonon if, during a LO-phonon emission time, scattering transfers little energy among carriers relative to the width of the peak. Thus at low densities the unrelaxed peak is unaffected by carrier-carrier scattering. At higher densities, however, the interactions among carriers are stronger, and at sufficiently high densities carrier-carrier scattering will reduce the height of the unrelaxed peak. The height of the unrelaxed peak thus allowed us to compare the relative importance of carrier-carrier scattering and LO-phonon emission for the scattering

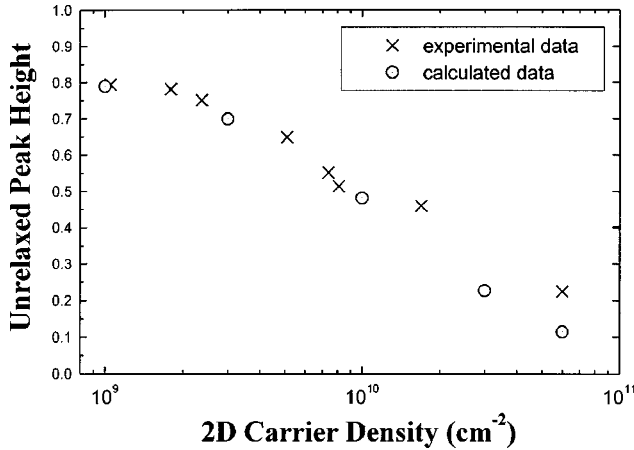

FIG. 3. Unrelaxed peak height vs carrier density as a function of carrier density. Experimental results are taken from data like that shown in Fig. 3. Calculated results are obtained by integrating the dynamically screened Boltzmann equation for 150 fsec.

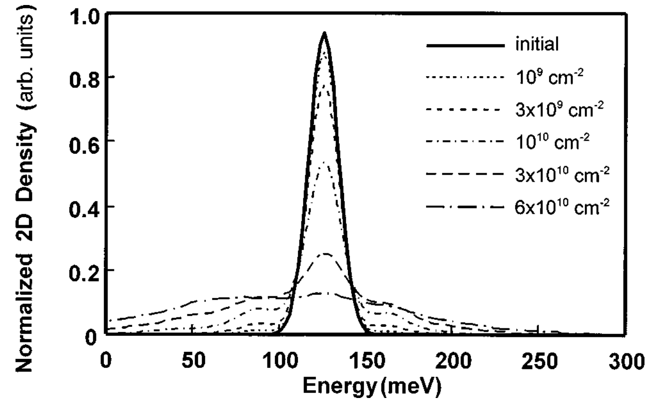

FIG. 4. The initial and final electron energy distribution in photoexcited 2D plasmas at densities from 10^9 to $6\times10^{10}\,cm^{-2}$, as calculated by integrating the dynamically screened Boltzmann equation for 150 fsec. All distributions are normalized to the total density.

of energetic electrons. We interpret the decrease of the unrelaxed peak height with increasing carrier density as evidence of the increasing importance of carrier-carrier scattering relative to LO-phonon scattering.

III. RESULTS OF CALCULATIONS

The method used for our calculations have been described previously.[19] Our calculations model a 2D layer of carriers in a single GaAs quantum well. The time evolution of the carriers is calculated using the 2D dynamically screened Boltzmann equation. The dynamic dielectric function includes the 2D carrier susceptibility, calculated in the random-phase approximation (RPA), and the Frohlich lattice susceptibility. Both electrons and holes are included. For simplicity we treat all holes as heavy holes, rather than partitioning the holes between heavy- and light-hole valence bands. This is expected to lead to a slight overestimate of the scattering rate in the calculations, since the in-plane effective mass of heavy holes ($m_{hh}=0.11m_0$) is more closely matched than the in-plane effective mass of light holes ($m_{lh}=0.23m_0$) to the in-plane electron effective mass ($m_e=0.0667m_0$). (The terms ''heavy hole'' and ''light hole'' refer to the 3D states from which the 2D states are derived; this accounts for the 2D heavy holes being lighter than the 2D light holes.) The energy of the incident photon is partitioned appropriately between electrons and heavy holes.

We model the 2D carriers in the quantum limit, as described in Ref. 19. This means that our calculations are based on a 2D Coulomb matrix element that is, strictly speaking, correct only for infinitely narrow quantum wells. The effect of quantum confinement is to increase the carrier-carrier scattering rate, and corrections to the quantum limit for finite well widths will modify the results in the direction of 3D behavior, i.e., slower scattering. Thus the use of the quantum limit is a second reason why the calculated results are expected to slightly overestimate the scattering rate that occurs in finite-width quantum wells.

The calculated evolution of the electron and hole distributions is followed for 150 fsec, the LO-phonon emission time. The initial and final electron distributions for various densities are shown in Fig. 4. The final distributions correspond to the unrelaxed peaks measured in our experiments. At higher densities sidebands can be observed in the final distributions, separated from the main peak by the 37 meV LO-phonon energy. These sidebands are rather small and have not been observed experimentally. They are due to resonant enhancement of the carrier-carrier scattering by the Frohlich lattice interaction, which yields a large cross section for scattering events that exchange the LO-phonon energy. Our calculations reproduce this effect because they include the dynamic lattice susceptibility in the dielectric function. We have observed this resonant enhancement in 3D calculations as well, but have found that it is very weak in 3D because changing an electron's energy by 37 meV involves a large momentum transfer, which is suppressed in 3D by the $1/q^4$ dependence of the squared Coulomb matrix element. In 2D, however, the squared matrix element has a $1/q^2$ dependence, rendering these 37 meV energy transfers more likely. Physically, this corresponds to the fact that lowering the dimensionality restricts the space available for glancing collisions, so that a larger fraction of the carrier collisions are close impacts in 2D than in 3D.

Figure 3 presents the results of our 2D scattering calculations with the experimental data. We have normalized the calculated final peak height at $10^9\,cm^{-2}$ to the measured peak height at this density, then applied the same scaling factor to the calculated peak heights at higher densities. The agreement between measured and calculated results is good. At densities higher than $10^{10}\,cm^{-2}$ the calculations predict more rapid scattering than is measured. As noted above, the approximations used in the calculations should lead to a slight overestimate in the calculated scattering. However, both measured and calculated results predict that at densities higher than about $10^{10}\,cm^{-2}$, carrier-carrier scattering becomes the dominant scattering process among 2D carriers.

IV. CONCLUSION

Our experimental results and our calculations show that at an injected carrier density of $10^9\,cm^{-2}$ the dominant scattering mechanism for photoexcited 2D electrons in GaAs quantum wells is LO-phonon emission. As the carrier density is

increased from 10^9 to $10^{11}\,cm^{-2}$, the carrier-carrier scattering rate increases, and at carrier densities greater than $10^{10}\,cm^{-2}$, carrier-carrier scattering is the dominant scattering process.

ACKNOWLEDGMENT

This work was supported by the National Science Council of Republic of China under Grant Nos. NSC87-2112-M-035-004 and NSC86-2112-M-035-008.

*Author to whom all correspondence should be addressed. FAX: 886-4-4510405. Electronic address: kwsun@fcu.edu.tw

[1] D. W. Snoke, W. W. Ruhle, Y. C. Lu, and E. Bauser, Phys. Rev. Lett. **68**, 990 (1992); Phys. Rev. B **45**, 10979 (1992).

[2] A. Leitenstorfer, C. Furst, Alaubereau, and W. Kaiser, Phys. Rev. Lett. **76**, 1545 (1996).

[3] J. L. Oudar, D. Hulin, A. Migus, A. Antonetti, and F. Alexandre, Phys. Rev. Lett. **55**, 2074 (1985).

[4] W. Knox, C. Hirlimann, D. A. B. Miller, J. Shah, D. S. Chemla, and C. V. Shank, Phys. Rev. Lett. **56**, 1191 (1986).

[5] J. P. Foing, D. Hulin, M. Joffre, M. K. Jackson, J. L. Oudar, C. Tanguy, and M. Combescot, Phys. Rev. Lett. **68**, 110 (1992).

[6] C. V. Shank, R. L. Fork, R. F. Leheny, and J. Shah, Phys. Rev. Lett. **42**, 112 (1979).

[7] J. F. Ryan, R. A. Taylor, A. J. Turberfield, A. Maciel, J. M. Worlock, A. C. Gossard, and W. Wiegmann, Phys. Rev. Lett. **53**, 1841 (1984).

[8] T. Elsaesser, J. Shah, L. Rota, and P. Lugli, Phys. Rev. Lett. **66**, 1757 (1991).

[9] J. Shah, B. Deveaud, T. C. Damen, W. T. Tsang, A. C. Gossard, and P. Lugli, Phys. Rev. Lett. **59**, 2222 (1987).

[10] K. W. Sun, M. G. Kane, and S. A. Lyon, Europhys. Lett. **26**, 123 (1994).

[11] A. Leitenstorfer, T. Elsaesser, F. Rossi, T. Kuhn, W. Klien, G. Boehm, G. Traenkle, and G. Weimann, Phys. Rev. B **53**, 9876 (1996).

[12] G. Fasol, W. Hackenberg, H. P. Hughes, K. Ploog, E. Bauser, and H. Kano, Phys. Rev. B **41**, 1461 (1990).

[13] B. P. Zakharchenya, V. D. Dymnikov, I. Ya. Karlik, and I. I. Reshina, J. Phys. Soc. Jpn. **49**, 573 (1980).

[14] J. A. Kash, J. M. Hvam, and J. C. Tsang, Phys. Rev. Lett. **54**, 2151 (1985).

[15] B. P. Zakharchenya, D. N. Mirlin, V. I. Perel, and I. I. Reshina, Usp. Fiz. Nauk [Sov. Phys. Usp. **25**, 143 (1982)].

[16] J. A. Kash, Phys. Rev. B **48**, 18336 (1993).

[17] W. H. Knox, D. S. Chemla, G. Livescu, J. E. Cunningham, and J. E. Henry, Phys. Rev. Lett. **61**, 1290 (1988).

[18] W. H. Knox, Solid-State Electron. **32**, 1057 (1989).

[19] M. G. Kane, Phys. Rev. B **54**, 16345 (1996).

[20] B. P. Zakharchenya, P. S. Kop'ev, D. N. Mirlin, D. G. Polakov, I. I. Reshina, V. F. Sapega, and A. A. Sirenko, Solid State Commun. **69**, 203 (1989).

[21] C. V. Shank, R. L. Fork, R. Yen, J. Shah, B. I. Greene, A. C. Gossard, and C. Weisbuch, Solid State Commun. **47**, 981 (1983).

[22] J. Shah, IEEE J. Quantum Electron. **QE-22**, 1728 (1986).

[23] S. A. Lyon, Superlattices Microstruct. **3**, 261 (1987).

[24] D. N. Mirlin and V. I. Perel', Semicond. Sci. Technol. **7**, 1221 (1992).

[25] D. Collings, K. L. Schumacher, F. Raksi, H. P. Hughes, and R. T. Philips, Appl. Phys. Lett. **64**, 889 (1994).